

27. Crystal Structures of Two Modifications of [3,*O*-Didehydro-MeBmt¹,Val²]-cyclosporin and Comparison of Three Different X-Ray Data Sets

by Ehmke Pohl, Regine Herbst-Irmer, and George M. Sheldrick*

Institut für Anorganische Chemie der Universität Göttingen, Tammannstrasse 4, D-37077 Göttingen

and Zbigniew Dauter and Keith S. Wilson

European Molecular Biology Laboratory (EMBL), c/o DESY, Notkestrasse 85, D-22603 Hamburg

and Johann J. Börlsterli, Pietro Bollinger, Jörg Kallen, and Malcolm D. Walkinshaw

Preclinical Research Department, Sandoz Ltd., CH-4002 Basel

(10.X.94)

The crystal structure of [3,*O*-didehydro-MeBmt¹,Val²]cyclosporin (PSC-833; **1**) was investigated by X-ray analysis. Data were collected from two different crystal modifications. Modification I crystallizes in *P*3₁21, $a = b = 21.419$ (2) Å, $c = 32.101$ (3) Å with one molecule in the asymmetric unit, modification II in *P*3₂21, $a = b = 21.313$ (2) Å, $c = 62.053$ (3) Å with two molecules per asymmetric unit. This non-immunosuppressive analogue of cyclosporin A adopts a similar backbone conformation to that found in the crystal structure of cyclosporin A and other analogues. Three different data sets of modification I were collected using an *Enraf-Nonius-CAD4* diffractometer with CuK_α radiation at 20°, a *Stoe-Siemens* four-circle diffractometer with MoK_α radiation at -120°, and an EMBL image-plate scanner with synchrotron radiation at 12°. The quality of the data sets was evaluated by internal consistency, independent structure solution, and refinement. The structural parameters reported here for modification I are based on the synchrotron data.

Introduction. – PSC-833, *i.e.*, [3,*O*-Didehydro-MeBmt¹,Val²]cyclosporin (**1**; *Fig. 1*) is a non-immunosuppressive analogue of the drug cyclosporin A (*Sandimmune*[®]). Cyclosporin A belongs to a family of undecapeptide fungal metabolites which have a wide

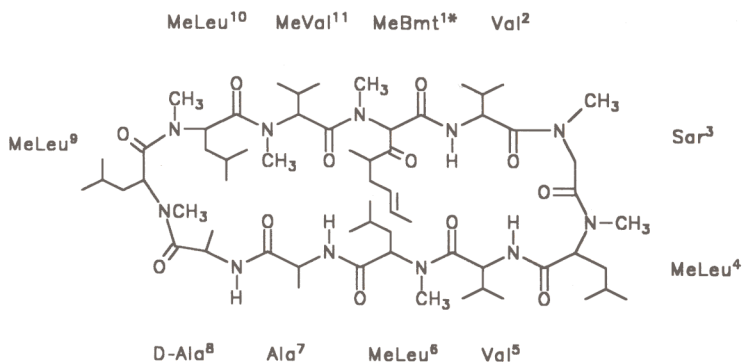


Fig. 1. Chemical constitution of PSC 833 (**1**). MeBmt^{*} = 3,*O*-didehydro-MeBmt.

spectrum of biological activities with therapeutic indication in allograft rejection, rheumatoid arthritis, and psoriasis [1] [2]. The biological mechanism for its immunosuppressive activity involves the formation of a complex between cyclosporin A and cyclophilin, an intracellular 18 kD protein [3] [4]. This cyclophilin-cyclosporin A complex further binds and inhibits the phosphatase, calcineurin thereby blocking the signal transduction pathway in T-lymphocytes and preventing T-cell proliferation [5]. Very small chemical modifications to cyclosporin A can have a profound effect on its biological activity [6], either affecting the binding to cyclophilin or reducing the binding and inhibition of calcineurin. The OH–C(3.1)¹⁾ to O=C(3.1)¹⁾ modification in PSC-833 (**1**) destroys the immunosuppressive effect of this derivative which is consistent with its inability to bind to cyclophilin [7].

A second and as yet little understood activity of cyclosporin A is its ability to induce multi-drug resistance. In various forms of chemotherapy, particularly in the treatment of cancer, a resistance is built up, and drug molecules are actively transported out of the cell. The mechanism is not fully understood, but the phenomenon was correlated with the overexpression of the transmembrane P-glycoproteins [8]. PSC-833 (**1**) was found to sensitize multi-drug-resistant cells *in vitro* and is ten times more active than cyclosporin A [7]. This multi-drug-resistance property coupled with a lack of immunosuppression makes **1** an interesting drug candidate for use in anti-cancer therapy.

Here we report the X-ray crystal structure of **1**. Two crystal modifications obtained under different crystallization conditions were investigated. Three different data sets of modification I were collected from similar crystals, using an *Enraf-Nonius-CAD4* diffractometer with CuK_α radiation at 20°, a *Stoe-Siemens* four-circle diffractometer with MoK_α radiation at –120°, and an EMBL image plate scanner with synchrotron radiation from the DORIS storage ring at *DESY*, Hamburg, at 12°. These data sets were used for a comparison of the quality of the data, evaluated by the internal consistency and by individual refinement of each data set. The ability of direct methods to solve the structure was also investigated using each data set independently.

Results and Discussion. – *Crystal Structure of PSC-833 (1)*. Crystal modification I is trigonal, space group *P*3₂1, with one peptide molecule in the asymmetric unit. The crystal structure and the numbering of the peptide backbone are shown in *Fig. 2*; a stereoview of the molecule with 50% probability displacement ellipsoids is shown in *Fig. 3*. Selected bond lengths and angles are given in *Table 1*. Modification II crystallizes

Table 1. Selected Bond Lengths [Å] and Angles [°] of Modification I of **1**. For numbering, see *Fig. 2*.

N(1)–C(1A)	1.461(5)	C(1A)–C(1)	1.513(5)
C(1)–O(1)	1.220(4)	C(1)–N(2)	1.327(5)
N(2)–C(2A)	1.452(5)	C(2A)–C(2)	1.520(7)
C(2)–N(3)	1.326(7)	C(2)–O(2)	1.233(6)
N(3)–C(3A)	1.466(8)	C(3A)–C(3)	1.506(10)
C(3)–O(3)	1.231(8)	C(3)–N(4)	1.358(7)
N(4)–C(4A)	1.468(7)	C(4A)–C(4)	1.518(6)
C(4)–O(4)	1.231(5)	C(4)–N(5)	1.331(6)
N(5)–C(5A)	1.445(6)	C(5A)–C(5)	1.529(6)

¹⁾ In OH–C(3.1) and O=C(3.1), the first locant refers to the C-atom of MeBmt and the second one to the residue number.

Table 1 (cont.)

C(5)–O(5)	1.232(4)	C(5)–N(6)	1.339(5)
N(6)–C(6A)	1.473(5)	C(6A)–C(6)	1.494(7)
C(6)–O(6)	1.227(5)	C(6)–N(7)	1.323(7)
N(7)–C(7A)	1.450(7)	C(7A)–C(7)	1.510(8)
C(7)–O(7)	1.215(6)	C(7)–N(8)	1.347(7)
N(8)–C(8A)	1.422(6)	C(8A)–C(8)	1.519(8)
C(8)–O(8)	1.232(6)	C(8)–N(9)	1.356(6)
N(9)–C(9A)	1.464(8)	C(9A)–C(9)	1.538(8)
C(9)–O(9)	1.237(9)	C(9)–N(10)	1.329(9)
N(10)–C(10A)	1.450(9)	C(10A)–C(10)	1.541(7)
C(10)–O(10)	1.221(6)	C(10)–N(11)	1.349(6)
N(11)–C(11A)	1.483(5)	C(11A)–C(11)	1.508(6)
C(11)–O(11)	1.243(4)	C(11)–N(1)	1.334(5)
N(1)–C(1A)–C(1)	109.6(2)	C(1A)–C(1)–N(2)	115.9(3)
C(1)–N(2)–C(2A)	122.6(3)	N(2)–C(2A)–C(2)	106.1(3)
C(2A)–C(2)–N(3)	121.6(4)	C(2)–N(3)–C(3A)	115.8(4)
N(3)–C(3A)–C(3)	107.4(4)	C(3A)–C(3)–N(4)	118.6(7)
C(3)–N(4)–C(4A)	117.7(5)	N(4)–C(4A)–C(4)	110.4(5)
C(4A)–C(4)–N(5)	115.0(4)	C(4)–N(5)–C(5A)	122.7(4)
N(5)–C(5A)–C(5)	109.5(3)	C(5A)–C(5)–N(6)	119.6(3)
C(5)–N(6)–C(6A)	118.3(3)	N(6)–C(6A)–C(6)	108.9(3)
C(6A)–C(6)–N(7)	116.5(4)	C(6)–N(7)–C(7A)	124.1(4)
N(7)–C(7A)–C(7)	111.0(4)	C(7A)–C(7)–N(8)	115.2(5)
C(7)–N(8)–C(8A)	121.7(4)	N(8)–C(8A)–C(8)	109.4(4)
C(8A)–C(8)–N(9)	118.2(5)	C(8)–N(9)–C(9A)	118.6(5)
N(9)–C(9A)–C(9)	111.0(5)	C(9A)–C(9)–N(10)	121.4(7)
C(9)–N(10)–C(10A)	126.2(5)	N(10)–C(10A)–C(10)	110.4(5)
C(10A)–C(10)–N(11)	117.7(5)	C(10)–N(11)–C(11A)	117.7(4)
N(11)–C(11A)–C(11)	109.0(3)	C(11A)–C(11)–N(1)	120.1(3)

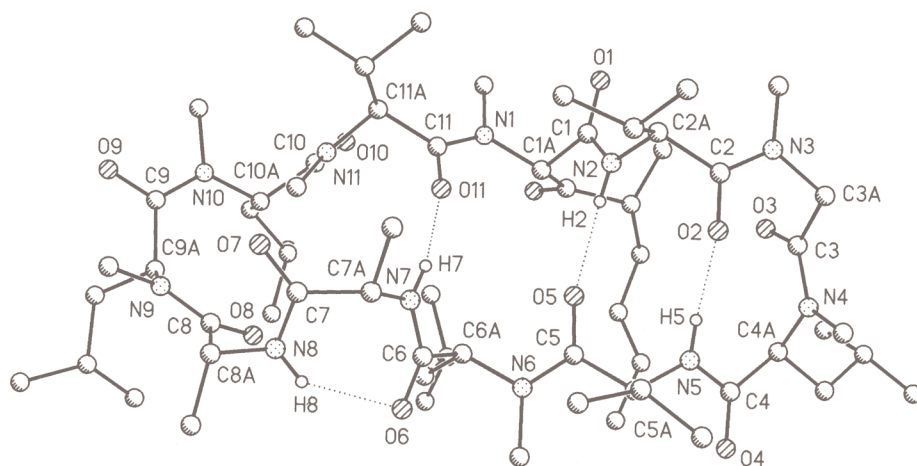


Fig. 2. Crystal structure of PSC-833 (1; modification I). H-Atoms except those involved in H-bonds have been omitted for clarity. Arbitrary numbering, locants refer to the residue number.

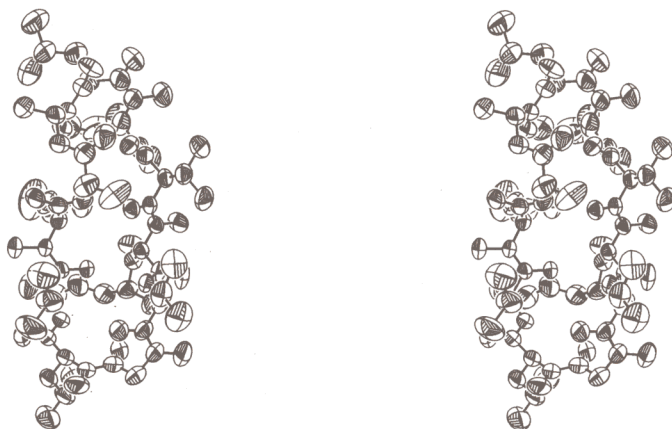


Fig. 3. Stereoview of modification I of **1** showing anisotropic displacement ellipsoids at 50% probability level

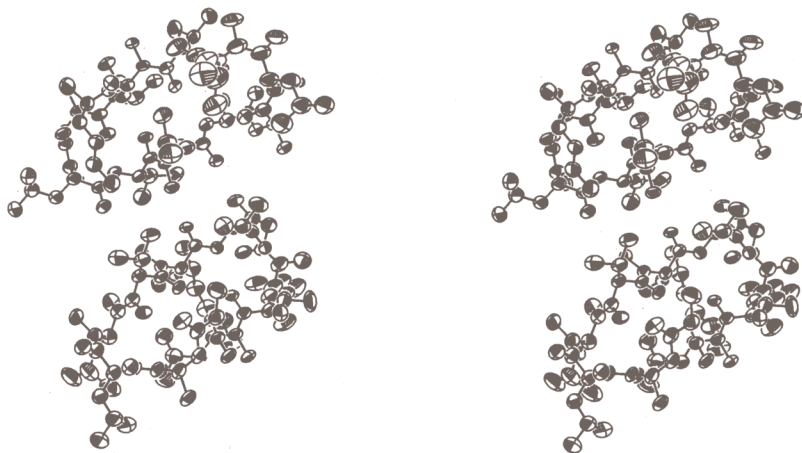


Fig. 4. Stereoview of modification II of **1** showing anisotropic displacement ellipsoids at 50% probability level

in the trigonal space group $P3_221$ with almost identical cell constants, except for a doubled c -axis. In this modification, there are two independent peptide molecules per asymmetric unit; they possess almost identical conformations to that of modification I. Therefore, selected bond lengths and angles and torsion angles are only given for modification I. A stereoview of modification II with 50% probability displacement ellipsoids is shown in *Fig. 4*. Crystal data of the two modifications are given in *Table 2*.

The residues 1–6 form an antiparallel β -pleated sheet stabilized by three H-bonds $N(2)-H(2)\cdots O(5)$, $N(5)-H(5)\cdots O(2)$, and $N(7)-H(7)\cdots O(11)$. A β -II' turn [9] is formed by the residues 2–5. Residues 7–11 form an open loop with the unusual H-bond $N(8)-H(8)\cdots O(6)$. The geometry of the H-bonds is summarized in *Table 3*. The ϕ , ψ , and ω torsion angles of the backbone are given in *Table 4*.

Table 2. Crystal Data for the Two Crystal Modifications I and II of 1

	Modifi- cation I	Modifi- cation II		Modifi- cation I	Modifi- cation II
Empirical formula	C ₆₉ H ₁₂₅ N ₁₁ O _{13.5}	C ₆₃ H ₁₁₁ N ₁₁ O ₁₂	2θ Range	2–41	8–38
Formula weight [g/mol]	1324.80	1214.63	No. of reflections	13918	13107
Crystal size [mm]	1.5 × 0.3 × 0.3	1.0 × 0.5 × 0.4	Independent	8753	12913
Temperature [°]	12	–120	R _{int}	0.041	0.089
Space group	P3 ₁ 21	P3 ₂ 21	No. of data	8742	12877
a [Å]	21.419(2)	21.313(2)	No. of restraints	285	2275
b [Å]	21.419(2)	21.313(2)	No. of parameters	894	1567
c [Å]	32.101(3)	62.053(3)	Goodness of fit S ^{a)}	1.093	1.098
V [Å ³]	12754(2)	24411(3)	wR2 (all data) ^{b)}	0.204	0.394
Z	6	12	R1 (F > 4σ(F)) ^{c)}	0.071	0.118
ρ _{calc} [Mgm ⁻³]	1.035	0.991	g ₁ , g ₂	0.1484, 0.8875	0.2, 90
μ [mm ⁻¹]	0.072	0.069	Max. [eÅ ⁻³]	0.353	0.508
F(000)	4344	7944	Min. [eÅ ⁻³]	–0.311	–0.285

^{a)} $S = [\Sigma[w(F_o^2 - F_c^2)^2]/(n - p)]^{1/2}$. ^{b)} $wR2 = [\Sigma[w(F_o^2 - F_c^2)^2]/\Sigma[w(F_o^2)^2]]^{1/2}$; $w^{-1} = \sigma^2(F_o)^2 + (g_1 \cdot P)^2 + g_2 \cdot P$, where $P = (F_o^2 + 2F_c^2)/3$. ^{c)} $R1 = \Sigma||F_o| - |F_c||/\Sigma|F_o|$ for $F > 4\sigma(F)$.

Table 3. Geometry of the Intramolecular H-Bonds in Modification I of 1. For numbering, see Fig. 2.

	D...A [Å]	D–H...A [°]
N(2)–H(2)···O(5)	2.912(4)	167.58(12)
N(5)–H(5)···O(2)	3.035(5)	154.75(14)
N(7)–H(7)···O(11)	2.907(4)	166.33(13)
N(8)–H(8)···O(6)	2.882(5)	143.64(14)

Table 4. Torsion Angles of the Peptide Backbone of Modification I of 1

	φ	ψ	ω
MeBmt ^{1*} a)	–94.6(4)	123.9(4)	177.3(3)
Val ²	–118.6(4)	112.5(5)	–178.0(4)
MeSar ³	61.4(8)	–132.5(6)	–172.2(5)
MeLeu ⁴	–115.2(5)	46.7(6)	175.3(5)
Val ⁵	–123.7(5)	138.4(4)	173.6(5)
MeLeu ⁶	–93.6(4)	115.9(4)	166.7(4)
Ala ⁷	–82.6(6)	61.8(6)	–178.5(4)
D-Ala ⁸	81.7(6)	–137.1(4)	–174.2(4)
MeLeu ⁹	–121.2(6)	106.6(7)	–167.9(4)
MeLeu ¹⁰	–137.3(6)	62.5(6)	–1.4(10)
MeVal ¹¹	–92.3(4)	121.8(4)	–174.8(4)

^{a)} MeBmt* = 3, O-Didehydro-MeBmt, see Fig. 1.

All peptide bonds are *trans* except the bond between residues 9 and 10 which is *cis*. The conformations of the alkyl side chains are generally staggered. The MeBmt* side chain is folded over the peptide backbone. The overall shape of the molecule is globular and compact. The bond lengths and angles compare well with those found in other cyclic peptides [10].

The crystal structure of modification II shows the same backbone conformation with minor variations in the conformations of the side chains. The two independent molecules in modification II differ from each other only in the orientation of the leucine side chains (residue 6). A least-squares fit of the 33 ring atoms has a r.m.s. deviation of 0.08 Å and is shown in *Fig. 5*. The superposition of modification I and one molecule of modification II is given in *Fig. 6* (r.m.s. deviation 0.12 Å).

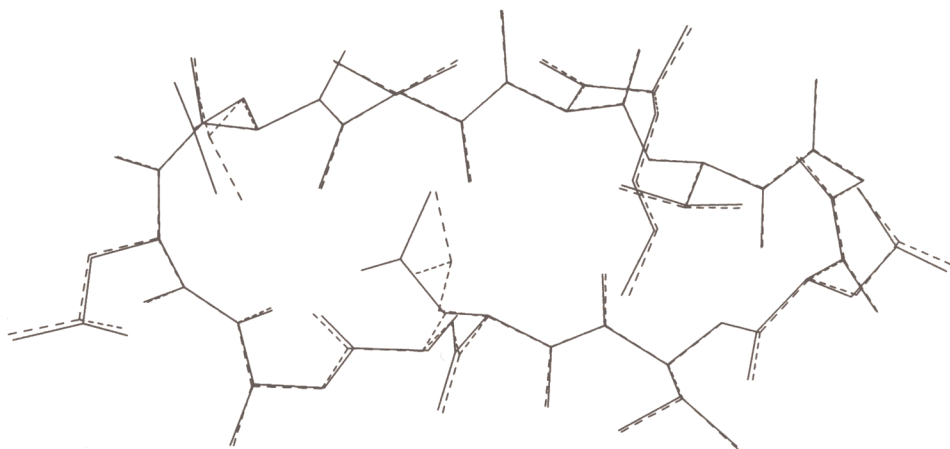


Fig. 5. Least-squares fit of the 33 ring atoms of two independent peptide molecules of modification II of **1**

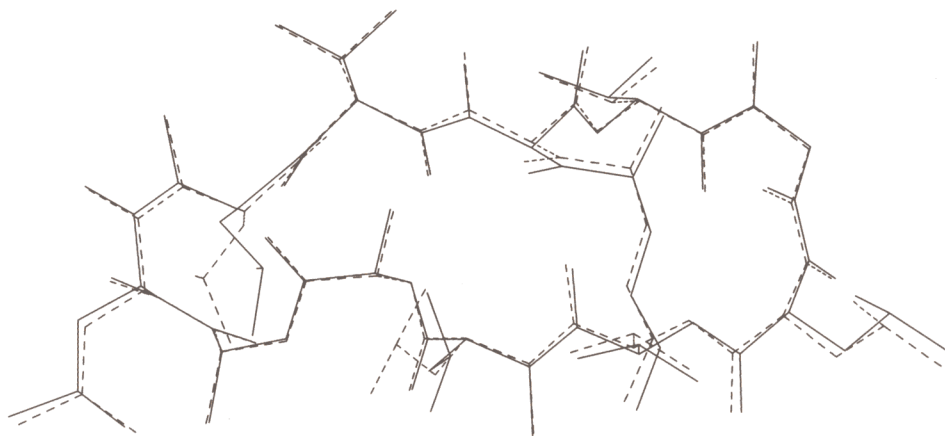


Fig. 6. Least-squares fit of modification I to one molecule of modification II of **1**

The structure of **1** (modification I) is very similar to the previously reported structure of cyclosporin A [11]. The superposition (*Fig. 7*) shows that the backbone conformations agree very well; the r.m.s. deviation of the backbone atoms is 0.49 Å. The conformation of the side chains is similar too, but there are some differences in the conformation of the

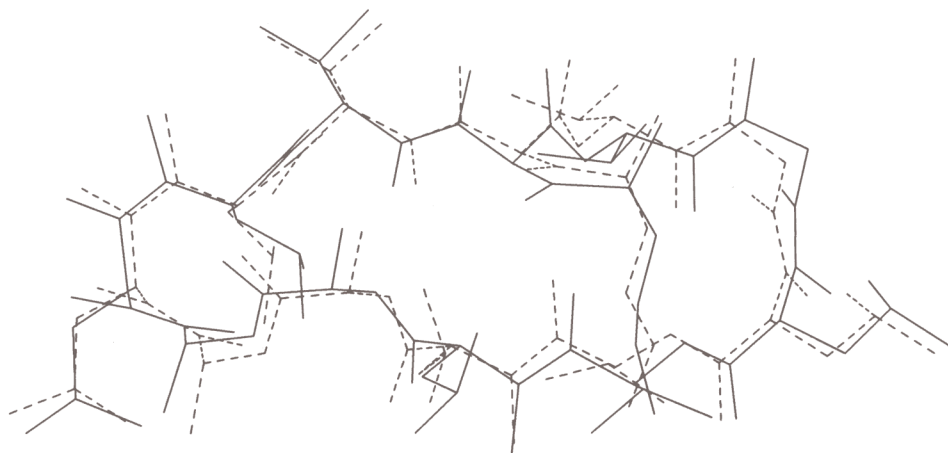


Fig. 7. Least-squares fit of PSC 833 (**1**; modification I) to cyclosporin A

MeBmt* side chain, because it contains a carbonyl group instead of an OH group in cyclosporin A. The same intramolecular H-bonds are found in the structures of **1** and cyclosporin A. These H-bonds hold the structure together and are responsible for the rigid backbone. Very similar backbone conformations were also found in the crystal structures of iodocyclosporin [12] and the dithio analogue [$^4\psi^5$,CS–NH; $^7\psi^8$,CS–NH]-cyclosporin A [13].

In apolar solvents (e.g. CDCl_3 , C_6D_6), an almost identical backbone conformation to that in the crystal structure was found by NMR techniques for cyclosporin A. In solvents of higher polarity, NMR studies indicated that many different conformations are present (e.g. in dimethylsulfoxide (DMSO), seven conformations can be observed) [14]. This may be due to a breaking of the intramolecular H-bonds and the forming of H-bonds to the solvent molecules.

The structure of cyclosporin A complexed with its cognate intracellular receptor protein cyclophilin was determined for two different crystal forms [3] and in solution by NMR [15]. All three structures showed a very similar conformation which is dramatically different from the conformations of PSC-833 (**1**) and cyclosporin A in uncomplexed crystals. The cyclophilin-bound conformation of cyclosporin A has all amide bonds *trans*, and there is no antiparallel sheet structure. The only intramolecular H-bond in this bound conformation is between the OH group of the MeBmt¹ side chain and the carbonyl O-atom of MeLeu⁴. Such a H-bond is not possible in the keto derivative **1** and probably explains why such a small chemical modification prevents binding to cyclophilin and, therefore, eliminates the immunosuppressive effect.

The crystal packing of modification I of **1** is shown in Fig. 8; there is a channel in the crystal filled with disordered solvent molecules, in which one diisopropyl ether molecule could be identified. The two largest residual electron-density peaks near a crystallographic two-fold axis were refined as O-atoms of H_2O molecules. No short contacts or H-bonds between the solvent molecules, the H_2O positions, or the peptide were found. Crystallographically identical crystals of modification I were also obtained by crystallization from tetrahydrofuran at 4° or by cooling a solution of **1** in DMSO/ H_2O from 40° to

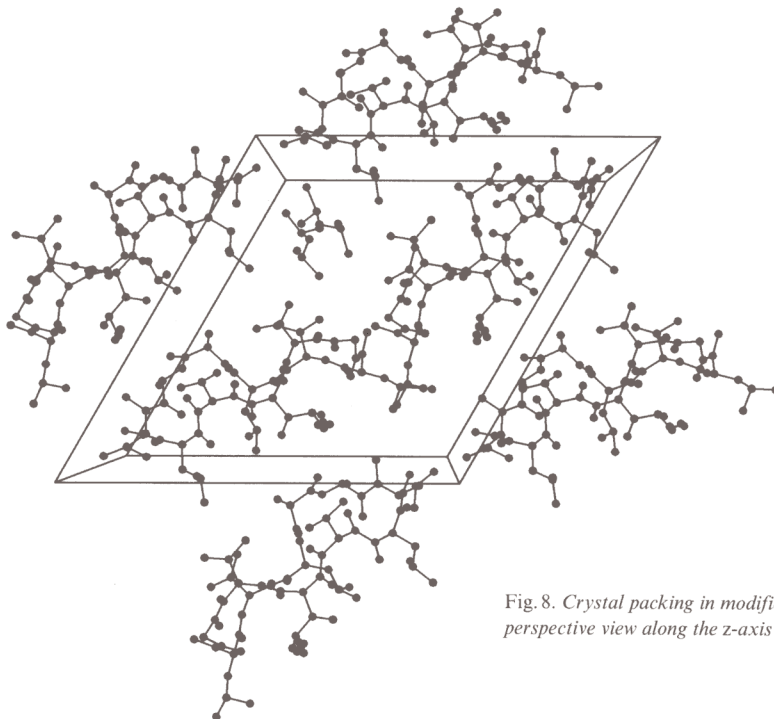


Fig. 8. Crystal packing in modification I of **1**: perspective view along the z-axis

room temperature within two weeks. We suggest that the channel can be filled with various solvent molecules without significant changes in the peptide conformation.

Comparison of the Three Data Sets for Modification I. The three data sets of modification I were collected, because we did not succeed in solving the structure using the *CAD4* and the *Stoe* diffractometer data sets which were collected first. With the synchrotron data, the structure was easily solved at essentially the first attempt using the phase-annealing approach implemented in SHELXS-90 [16]. After *E-Fourier* recycling of the best solution, every atom of the peptide molecule was present in the final *E*-map.

To compare the quality of the different data sets, we first evaluated the internal consistency by calculating the R_{int} values within each data set (symmetry equivalents had already been merged during the data reduction for the *CAD4* data); no significant *Bijvoet* differences would be expected for this structure. The lowest R_{int} value was obtained for the synchrotron data (0.041), whereas the *Stoe* data resulted in a slightly higher R_{int} value (0.052). As the R_{int} values depend on the redundancy of data and of the different scaling algorithms used during data processing, we applied a further test for the data quality. Each data set was refined on F^2 individually using the refinement program SHELXL-93 [17]. We suggest that this is a more objective test of the data quality than the R_{int} values.

The resulting structures were almost identical. The r.m.s. deviations of the least-squares fits of the 33 ring atoms were less than 0.1 Å, but there were differences in the precision of the refined structures. The lowest overall *R* factors and parameter e.s.d.'s (see *Table 5*) were obtained using the synchrotron data, the values for the low-temperature *Stoe* diffractometer data being only slightly higher, whereas for the room-temperature

Table 5. Data Collection and Refinement Parameters for the Three Data Sets of Modification I

	Synchrotron	Stoe	CAD4
X-Ray source	synchrotron	sealed tube	sealed tube
Wavelength [Å]	0.700	0.71073	1.5478
[kV, mA]	–	55, 30	45, 32
Crystal size [mm]	1.5 × 0.3 × 0.3	1.0 × 0.3 × 0.3	1.0 × 0.3 × 0.3
Temperature [°]	12	–120	20
μ [mm ⁻¹]	0.072	0.072	0.578
2 θ -Range [°]	2–41	8–43	5–140
Index ranges ^{a)}			
<i>h</i>	0 < <i>h</i> < 21	–19 < <i>h</i> < 19	–11 < <i>h</i> < 24
<i>k</i>	–19 < <i>k</i> < –16	–19 < <i>k</i> < 19	–12 < <i>k</i> < 24
<i>l</i>	–32 < <i>l</i> < 32	–32 < <i>l</i> < 32	0 < <i>l</i> < 39
No. of reflections ^{b)}	13918	14856	10663
Independent	8753	8722	10663
Used for refinement	8742	8716	10652
R_{int} ^{b)}	0.041	0.0518	–
Resolution [Å]	0.89	1.0	0.85
No. of data	8742	8716	10652
No of parameters	894	894	893
Restraints	285	279	273
$R1$ ($F > 4\sigma(F)$)	0.071	0.074	0.113
$wR2$ (all data)	0.204	0.219	0.315
Ext. coeff.	0.0028(6)	0.0068(9)	–
Diff. elect. dens.			
max. [eÅ ⁻³]	0.353	0.363	0.238
min. [eÅ ⁻³]	–0.311	–0.252	–0.224
E.s.d.'s for			
distances [Å]	0.006–0.010	0.006–0.012	0.007–0.017
angles [°]	0.4–0.9	0.4–0.9	0.5–1.4

^{a)} Not all reflections within these ranges were measured. ^{b)} After data processing, *Friedel* opposites not merged.

CAD4 data, these values were significantly higher. Since on the evidence of the refinement, the synchrotron data are clearly best, they were used for the final refined structural parameters reported here and deposited.

The failure of direct methods [16] to solve the structure using the two diffractometer data sets is surprising for a structure of this size. In the case of the *CAD4* data, the poorer quality of the high-resolution data may have been responsible; in the case of the *Stoe* four-circle data, missing low-angle data may be the problem. For reasons involving the low-temperature device, the minimum 2 θ angle was set to 8°, with the result that all reflections below a 2 θ angle of 8° are missing from the *Stoe* data set. The synchrotron data (better beam collimation) and *CAD4* data (longer wavelength) are remarkably complete at low angle, missing only 6 and 4% unique data, in this range, respectively.

The low-angle reflections play an important role in direct methods, because they enter into many phase relations. It proved impossible to solve the structure with the synchrotron data when these low-angle reflections with 2 θ < 8° were not used.

We gratefully acknowledge financial support from the *Deutsche Forschungsgemeinschaft* and the *Fonds der Chemischen Industrie*.

Experimental Part

Preparation and Crystallization of PSC-833 (I). PSC-833 ($[3, O\text{-didehydro-MeBmt}^1, \text{Val}^2]\text{cyclosporin}$; **1**) was prepared in one step from $[\text{Val}^2]\text{cyclosporin}$ (cyclosporin D) by oxidation. PSC-833 is a neutral substance soluble in EtOH and DMSO but insoluble in H_2O . Colorless crystals of modification I were obtained from $(i\text{-Pr})_2\text{O}$ at r.t. Crystallographically identical crystals were obtained from THF at 4° or by cooling a soln. in DMSO/ H_2O from 40° to r.t. within 2 weeks. These crystals were of lower quality, so no data were collected from them. Crystals of modification II were obtained by slow evaporation of a soln. in pentane/ CH_2Cl_2 at r.t.

Data Collection and Processing. Crystal data are summarized in Table 2; data collection parameters and refinement parameters for the comparison are given in Table 5. The synchrotron data were collected on the X31 EMBL beam-line located on the DORIS storage ring at DESY, Hamburg. The ring was operating at 5.7 GeV with electrons running in multi-bunch mode. The EMBL imaging-plate scanner was used as a detector. The strategy of data collection on the scanner was based on the rotation method developed for photographic film [18], with oscillation ranges as wide as the crystal cell dimensions and the maximum resolution permitted, whilst avoiding spatial overlap of reflections recorded on the image plate. The intensities were collected in three passes from the same crystal, at high, medium, and low resolution, at crystal to detector distances of 100, 220, and 350 mm with ϕ -increments of 1, 2, and 5° using different exposure times. Multiple passes were needed because the stronger (low resolution) reflections saturated the scanner electronic read-out system, and some pixels were thus unmeasurable when the exposure time was sufficiently long to obtain significant intensities from weaker, high-resolution reflections. Every image after exposure was scanned automatically and stored on the disk for processing off-line. Data collection parameters are summarized in Table 5. The crystal was oriented so that its c -axis was roughly at 20° from the spindle axis, thus minimizing the number of unique reflections in the 'blind region' near the rotation axis which cannot cross the surface of the Ewald sphere. For every pass, the crystal was rotated by a total of ca. 70° to ensure high redundancy of the data (with c -axis along the spindle, the asymmetric unit is 30°). The wavelength used was 0.700 \AA , and no absorption or decay corrections were applied. The images were subsequently processed with the program DENZO [19], scaled and merged to give the unique set of intensities. Only fully recorded reflections were accepted from each image; because of the high completeness, no attempt was made to use the sums of partially recorded intensities from pairs of successive images. Accurate cell dimensions were obtained by least-squares from the same crystal on a *Stoe-Huber* four-circle diffractometer with graphite-monochromated MoK_α radiation with 50 reflections centered at $+2\theta$, $+\omega$ and -2θ , $-\omega$ in the 2θ range of 20 to 25° . These cell dimensions were used for all refinements, because the cells determined at low temperature and with the *CAD4* system were less accurate.

The *Stoe* data were collected on a four-circle diffractometer with graphite-monochromated MoK_α radiation (λ 0.71073 \AA). The crystal was mounted on the tip of a glass fibre using the 'oil-drop' method where the crystal is mounted in an inert oil [20]. The crystal was cooled to -120° by a cold N_2 stream with a locally built low-temperature device [21]. Intensities were obtained from ω - 2θ scans with variable scan speed by a 'learnt profile' method [22].

The *CAD4* data were collected with an *Enraf-Nonius CAD4* diffractometer with graphite-monochromated CuK_α radiation (λ 1.5478 \AA) at r.t. [23]. The intensities were obtained from three crystals of the same size which were mounted in *Lindemann* glass capillaries. Data processing was performed using the program CADABS [24].

Data of crystal modification II were collected on a *Stoe-Siemens* four-circle diffractometer at -120° by the method described above for the *Stoe* four-circle data of modification I.

Structure Solution and Refinement. Crystal Modification I. The structure was solved by direct methods using the synchrotron data and SHELXS-90 [16]. All non-H-atoms were refined anisotropically against F^2 by full-matrix least-squares method with SHELXL-93 [17]. H-Atoms were included in calculated positions and refined assuming a riding model. Similarity restraints were applied to the chemically equivalent 1,2- and 1,3-distances of all the leucine residues. The side chain of residue 10 was found to be disordered. Two sets of positions (C(10B) to C(10E) and C(10F) to C(10I)) were refined to occupancies of P and $1-P$, respectively (P refined to 0.65 for the synchrotron data). These atoms were refined using rigid-bond restraints [25] on the anisotropic displacement parameters of 1,2- and 1,3-atom pairs, and similarity restraints (approximately equal U_{ij}) to atoms closer than 1.2 \AA to each other. These restraints lead to more reasonable values for the bond lengths and angles. For the *Stoe* data and the synchrotron data, an extinction correction was found to be necessary [26].

Crystal Modification II. As a result of the systematically weaker reflections with l odd, the percentage of observed reflections [$F > 4\sigma(F)$] in the critical $1.1\text{--}1.2 \text{ \AA}$ range [16] was only 44%, so it is not surprising that exhaustive attempts with direct methods were not successful in solving this structure with almost 200 unique non-H-atoms. The structure was eventually solved by a new procedure which will be described in detail elsewhere

[27]. A rotation search to maximize the sum of $(E_0^2 - 1) \cdot E_c^2$ was performed for a 60-atom fragment from modification I (ring atoms plus those atoms directly attached). The best four unique orientations were subjected to partial structure-expansion cycles consisting of tangent expansion [28], *E-Fourier*, and 'peaklist optimization' [29] with the data expanded to space group *P*1. Starting from the initial model, 3 tangent formula iterations per cycle were performed, thereafter one iteration per cycle. This expansion was performed starting from the 2565 reflections with the largest E_c values chosen from the 5130 with $E_0 > 1.4$, and phases were generated for the 17560 $E_0 > 0.8$. All 38978 reflections (after expansion to *P*1) were used to choose the subset (*ca.* 1000) of the 1743 peaks which gave the highest correlation coefficient [30]. After 40 cycles, the best rotation solution had reached a correlation coefficient of 65%; by inspection of the peak coordinates, it was possible to deduce the correct space group (*P*3₂21 rather than *P*3₁21) and origin, and find all the atoms of the two independent molecules (after combining symmetry equivalents). The idea of real/reciprocal space alternation was inspired by the 'shake and bake' algorithm of Weeks *et al.* [31].

All non-H-atoms were refined anisotropically against F^2 by blocked-matrix least-squares using SHELXL-93. The H-atoms were included in calculated positions and refined using a riding model. Rigid-bond restraints (for 1,2 and 1,3 pairs) and 'similarity' restraints (for atoms closer than 1.7 Å) were applied to the anisotropic displacement parameters. The 1,2- and 1,3-distances of the two crystallographically independent but chemically equivalent molecules were restrained to have similar values, but the torsion angles were free to vary. The chemically equivalent distances of the four leucine, the two alanine, and two valine residues were also restrained to similar values. All carbonyl C-atoms were restrained to have a planar environment. These chemically reasonable restraints enabled a full anisotropic refinement despite rather weak data. The leucine residue 10 in one molecule was found to be disordered. Two positions for the methyl groups C(10D) and C(10E), C(10F) and C(10G) were refined to occupancies of *P* and 1-*P* (*P* = 0.65). The absolute structure was previously known.

Lists of observed and calculated structure factors, crystal data, fractional atomic coordinates, anisotropic displacement parameters, and full bond lengths and angles were deposited at the *Cambridge Crystallographic Data Center*.

REFERENCES

- [1] J. F. Borel, 'Pharmacology of Cyclosporine (Sandimmune) IV. Pharmacological Properties in Vivo', *Pharmacol. Rev.* **1989**, *41*, 259.
- [2] R. M. Wenger, *Angew. Chem.* **1985**, *97*, 88.
- [3] G. Pflügl, J. Kallen, T. Schirmer, J. N. Jansonius, M. G. M. Zurini, M. D. Walkinshaw, *Nature (London)* **1993**, *361*, 91; V. Mikol, J. Kallen, M. D. Walkinshaw, *J. Mol. Biol.* **1993**, *234*, 1119.
- [4] Y. Theriault, T. M. Logan, R. Meadows, L. Yu, E. T. Olejniczak, T. F. Holzmann, R. L. Simmer, S. W. Fesik, *Nature (London)* **1993**, *361*, 88.
- [5] S. L. Schreiber, G. R. Carbtree, *Immunol. Today* **1992**, *13*, 136.
- [6] N. H. Sigal, F. Dumont, P. Durette, J. J. Siejlerka, L. Peterson, D. H. Rich, B. E. Dunlap, M. J. Staruch, M. R. Melino, S. L. Koprak, D. Williams, B. Witzel, J. M. Pisano, *J. Exp. Med.* **1991**, *173*, 619.
- [7] C. Gaveriaux, D. Boesch, B. Jachez, P. Bollinger, T. Payne, F. Loor, *J. Cell. Pharmacol.* **1991**, *2*, 225.
- [8] M. G. M. Zurini, *TIPS* **1988**, *9*, 54.
- [9] J. A. Smith, L. G. Pease, *CRC Crit. Rev. Biochem.* **1980**, *8*, 315.
- [10] G. M. Sheldrick, J. J. Guy, O. Kennard, V. Rivera, M. J. Waring, *J. Chem. Soc., Perkin Trans.* **1984**, 1601; M. B. Hossain, D. van der Helm, J. Antel, G. M. Sheldrick, S. K. Sanduja, A. J. Weinheimer, *Proc. Natl. Acad. Sci. U.S.A.* **1988**, *85*, 4118; I. L. Karle, J. W. Gibson, J. Karle, *J. Am. Chem. Soc.* **1970**, *92*, 3755; M. B. Hossain, D. van der Helm, *ibid.* **1978**, *100*, 5191; I. L. Karle, B. K. Handa, C. H. Hassal, *Acta Crystallogr., Sect. B* **1975**, *31*, 555; I. L. Karle, J. Flippen-Anderson, *ibid.*, *Sect. C* **1990**, *46*, 303.
- [11] H. R. Loosli, H. Kessler, H. Oschkinat, H. P. Weber, T. J. Petcher, A. Widmer, *Helv. Chim. Acta* **1985**, *68*, 682.
- [12] T. J. Petcher, H. P. Weber, A. Rügger, *Helv. Chim. Acta* **1976**, *59*, 1480.
- [13] D. Seebach, S. Y. Ko, H. Kessler, M. Köck, M. Reggelin, P. Schmieder, M. D. Walkinshaw, J. J. Bölsterli, D. Bevec, *Helv. Chim. Acta* **1991**, *74*, 1953.
- [14] H. Kessler, M. Köck, T. Wein, M. Gehrke, *Helv. Chim. Acta* **1990**, *73*, 1818.
- [15] C. Weber, G. Wider, B. von Freyberg, R. Traber, W. Braun, H. Widmer, K. Wüthrich, *Biochemistry* **1991**, *30*, 6563; S. W. Fesik, R. T. Gampe, H. L. Eaton, G. Gemmecker, E. T. Olejniczak, P. Neri, T. F. Holzman, D. A. Egan, R. Edalji, R. Simmer, R. Helfrich, J. Hochlowski, M. Jackson, *ibid.* **1991**, *30*, 6574.

- [16] G. M. Sheldrick, *Acta Crystallogr., Sect. A* **1990**, *46*, 467.
- [17] G. M. Sheldrick, 'SHELXL-93, Program for Crystal Structure Refinement', University of Göttingen, 1993.
- [18] U. W. Arndt, A. J. Wonacott, Eds., 'The Rotation Method in Crystallography', North Holland, Amsterdam, 1977.
- [19] Z. Otwinowski, 'DENZO, Data Processing Program for Macromolecular Crystallography', Yale University, New Haven, 1991.
- [20] T. Kottke, D. Stalke, *J. Appl. Cryst.* **1993**, *26*, 615.
- [21] T. Kottke, Dissertation, Universität Göttingen, 1993.
- [22] W. Clegg, *Acta Crystallogr., Sect. A* **1981**, *37*, 22.
- [23] 'Enraf-Nonius Structure Determination Package', *Enraf-Nonius*, Delft, 1985.
- [24] R. O. Gould, D. E. Smith, 'Cadabs', University of Edinburgh, 1986.
- [25] J. S. Rollet, 'Crystallographic Computing', Eds. F. R. Ahmed, S. R. Hall, and C. P. Huber, Munksgaard, Copenhagen, 1970, p. 167; F. L. Hirshfeld, *Acta Crystallogr., Sect. A* **1976**, *32*, 239; K. N. Trueblood, J. D. Dunitz, *ibid.*, *Sect. B* **1983**, *39*, 120.
- [26] A. C. Larson, 'Crystallographic Computing', Eds. F. R. Ahmed, S. R. Hall, and C. P. Huber, Munksgaard, Copenhagen, 1970, p. 291.
- [27] G. M. Sheldrick, R. O. Gould, submitted to *Acta Crystallogr., Sect. A*.
- [28] J. Karle, *Acta Crystallogr., Sect. B* **1968**, *24*, 182.
- [29] G. M. Sheldrick, 'Crystallographic Computing', Ed. D. Sayre, Clarendon Press, Oxford, 1982, p. 506.
- [30] M. Fujinaga, R. J. Read, *J. Appl. Cryst.* **1987**, *20*, 517.
- [31] C. M. Weeks, G. T. DeTitta, H. A. Hauptman, P. Thuman, R. Miller, *Acta Crystallogr., Sect. A* **1994**, *50*, 210.